Hindawi
Advances in Civil Engineering
Volume 2020, Article ID 8837480, 15 pages
https://doi.org/10.1155/2020/8837480

Research Article

Application of Improved Single-Hole Superposition Theory in Nonequal Cross-Section Tunnel Intersection

Ning Liu,[1,2] **Yi-Xiong Huang**,[1] **Wei Cai**,[1] **and Kun Chen**[1]

[1]*School of Civil Engineering, Guizhou University, Guiyang, China*
[2]*College of Civil Engineering and Architecture, Guangxi University, Nanning, China*

Correspondence should be addressed to Ning Liu; nliu1@gzu.edu.cn

Received 3 September 2020; Revised 11 November 2020; Accepted 13 November 2020; Published 10 December 2020

Academic Editor: Mingfeng Lei

With the excavation towards the intersecting tunnels' direction, the impact on the surrounding rock stress between the two tunnels will gradually decrease, but how it decreased is not clear. At present, engineers often directly superimpose the stress in the triangular area of the crossing tunnel when calculating the stress in this area (single-hole superposition theory). The theory is also used as the main theory to consider the surrounding rock stress for support which is difficult to explain the situation of nonuniform cross-section centers not in the same plane. The safety level of support is mainly determined by construction experience which is unable to determine how to adjust the support level with the increase in the horizontal distance of intersecting tunnel, causing the insufficient utilization of materials. This paper derives theoretically the stress calculation of the triangular area of circular cross tunnels with different cross sections and analyzes the surrounding rock stress law of the intersecting tunnels triangular area from different cross-section dimensions (the difference in diameter between the two tunnels is twice, 3 times, and 4 times) and different intersection angles. And the results show that, compared with the case of equal tunnel diameters, the stress influence area of the surrounding rock in the triangle area mainly expands to the side of the small section with the increase of the cross-section difference of the intersecting tunnels; the dangerous area of the surrounding rock in the triangle area moves vertically to the small section; the safest condition is the two tunnels with 90° intersecting angle. The theoretical calculation model of this paper is verified by the previous research results.

1. Introduction

The land resource on the ground is becoming more and more rare since the rapid increase in the population of China. The construction scale of underground projects is becoming larger and the structural form is becoming more complex due to the diversification of the use functions. Therefore, the emergence of underground intersecting tunnels is inevitable. The research of stability of the surrounding rock at the intersection is the key point of the excavation of the underground tunnel, and the section size of the tunnel is an important factor. When the main cave and the auxiliary cave intersect with an acute angle, the stress concentration of the surrounding rock in the triangle area is greater than that which forms an obtuse angle, and the stability of the surrounding rock is poor. As the angle of intersection gradually changes to a vertical intersection, the surrounding rock becomes gradually stable [1].

For the stability of the surrounding rock in the triangle area of the intersection, scholars at home and abroad have also carried out a lot of researches. For example, Professor Ping [2] proposed a calculation method for the stability of the surrounding rock of the roadway at the intersection and put forward the theory named equivalent span and gave us the distribution curve of the concentration coefficient K. Sun [3] analyzed the vertical stress distribution law of the surrounding rock at the intersection under different spans and heights of the intersection roadway with Professor Ping's theory; Rao et al. [4] further summarized the vertical stress distribution law of surrounding rock at different angles between the main tunnel and the auxiliary tunnel at the intersection; Shi [5] introduced the deformation law of the surrounding rock of the roadway with different intersections and analyzed the formation mechanism of rock column pressure in the corners of the intersection; Singh [6] and

others carried out numerical simulation analysis on three-way intersection roadway and proposed the design criteria for three-way intersection support system; Professor Yoginder P. Chugh of Southern Illinois University, aiming at roadway roof fall accidents occurring at intersections, announced that proper selection and installation of the main support and auxiliary support around these areas can helpfully reduce the occurrence and expansion of the failure [7, 8]. Therefore, numerical simulation data are used to evaluate the roof support plan, and the method of rock reinforcement is used to improve the roof support around the intersection according to his conclusion. Hao Wu et al. [9] conducted a series of uniaxial compression tests on rocks with intersecting holes to simulate rocks with deep underground structures. Based on the test results, they figured out how the prefabricated cavity affects the mechanical properties of the specimen.

Liu et al. [10] conducted laboratory tests on the seismic response of spatial crossing tunnels, carried out numerical simulation studies, and summarized the ground motion acceleration response law at the intersection center of the tunnel. The intersection center under the mutual influence of the upper tunnel and the lower tunnel was analyzed. The vibration acceleration distribution of the section and the sorting of the acceleration of different parts of the section were analyzed. Lei et al. [11] analyzed and studied the tunnel construction risks of shield tunnels underneath the existing railway in sand and gravel stratum and put forward key risk factors such as sand and gravel stratum, grouting delay, and incorrect indoor earth pressure setting. A series of control measures have been adopted to prevent uncontrollable large deformation of the surrounding rock in the tunnel. At the same time, the influence law of soft clay intrusion thickness and atmospheric precipitation on tunnel surrounding rock deformation during the construction of high plastic soft clay tunnel is studied [12]. Based on EMI testing technology, Lei et al. [13] conducted laboratory tests on the mechanical properties of concrete members under impact load and summarized the damage mechanics laws of members under this type of environment.

Many studies have shown that scholars have made a lot of achievements on the stability of the surrounding rock at the intersection of underground tunnels, but there are few studies on the influence of the difference in the section of the tunnel on the deformation and stress law of the surrounding rock in the triangle area of the intersection. On the basis of the relational theory, this paper theoretically deduced and analyzed the problem of the obvious size difference of cross section of the intersection tunnel, compared the theoretical calculation from this paper with the numerical simulation and experimental data of the published papers, and provided theoretical support for the design and construction of similar projects.

2. Proposal of the Improvement Theory of the Triangular Area in the Intersection Tunnel

The triangle area will appear with the intersecting tunnel excavation (as shown in Figure 1). After the completion of the excavation, the surrounding rock stress will be redistributed and the stress concentration will be easily formed in the triangle area. However, the existing theory has certain limitations in calculating the stress in the triangle area. Therefore, this section will introduce how the new theory is put forward to the problem.

2.1. Limitations of the Existing Stress Calculation Theory. The surrounding rock is often broken in practical engineering due to excessive concentrated stress. To ensure the safety of construction, the stress distribution of surrounding rock in this area needs to be explored. Assuming that the rock mass is an elastomer, the tangential stress σ_θ around the portal of a deeply buried single-hole tunnel can be calculated by formula (1) [14]. As for circular intersecting tunnels with the same radius, the vertical stress σ_h in the intersection triangle can be calculated by formula (2) [2]:

$$\sigma_\theta = \frac{P(1+\lambda)}{2}\left(1+\frac{r_0^2}{r^2}\right)+\frac{P(1-\lambda)}{2}\left(1+\frac{3r_0^4}{r^4}\right)\cos 2\theta, \quad (1)$$

$$\begin{aligned}\sigma_h = {} & \frac{P(1+\lambda)}{2}\left[1+\frac{r_0^2}{(\rho\sin\theta+r_0)^2}\right] \\ & +\frac{P(1-\lambda)}{2}\left[1+\frac{3r_0^4}{(\rho\sin\theta+r_0)^4}\right] \\ & +\frac{P(1+\lambda)}{2}\left\{1+\frac{r_0^2}{[\rho\sin(\alpha-\theta)+r_0]^2}\right\} \\ & +\frac{P(1-\lambda)}{2}\left\{1+\frac{3r_0^4}{[\rho\sin(\alpha-\theta)+r_0]^4}\right\}.\end{aligned} \quad (2)$$

In the formula, σ_θ is the tangential stress of the single-hole tunnel; σ_h is the vertical stress of the surrounding rock in the triangular area of the intersecting tunnel; P is the original rock stress; λ is the lateral pressure coefficient; r_0 is the radius of the excavated tunnel; (ρ, θ) are the polar coordinates of the calculated points; α is the intersection angle of the two tunnels.

It can be known from formula (1) that the shear stress of a single-hole tunnel reaches the maximum at the positions of $\theta = 0$ and $\theta = 180^\circ$ on the circumference of the hole. At the same time, the direction of the maximum shear stress is perpendicular to the plane of the center of the circle and points downward. Therefore, Professor Ping proposed a calculation method of vertical stress shown in formula (2) by superimposing the tangential stress of two tunnels on the central plane of a circle.

It can be concluded from formula (2) that the maximum tangential stress on the horizontal plane of the two equal-radius intersecting single-hole circular tunnels is directly added (hereinafter referred to as the single-hole superposition theory) when calculating the stress of the surrounding rock in the triangle area. As long as the maximum shear stress is obtained and the corresponding support is carried out, the intersection triangle will be in a safe state. However, the limitation of this method is revealed: this method is only applicable to the situation when the centers of the two

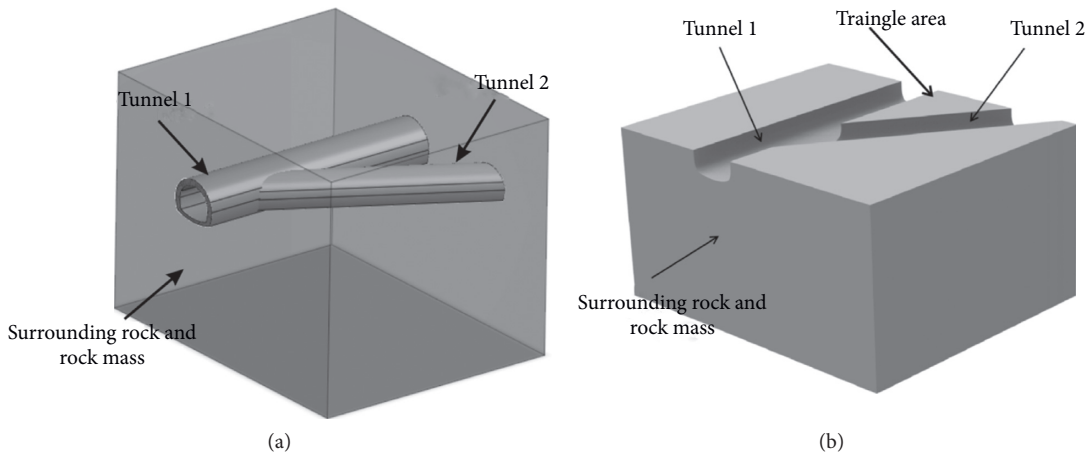

Figure 1: Schematic diagram of intersecting tunnels. (a) Cross tunnel. (b) Triangle area.

intersecting tunnels are in the same horizontal plane and is only applicable to calculate the tangential stress of the plane. The superposition calculation cannot be performed when there are obvious differences in cross sections and when the two different sizes of intersecting tunnels are not in one horizontal plane. Unfortunately, there is no effective stress calculation theory so far; the study can only be conducted with numerical simulation software.

2.2. Conception and Proposal of the Improved Theoretical Calculation Model. The intersecting tunnels are different from the double-hole parallel tunnels in dealing with the plane problem. Only to select the cross sections and treat them as a double-hole plane problem can solve the stress for the double-hole parallel tunnels. Therefore, the method to deal with intersecting tunnels is proposed in this paper. The intersecting tunnels are divided by multiple planes that are close together, as shown in Figure 2(a); each plane will divide the two sections of the intersecting tunnels, as shown in Figure 2(b). And the two holes on each plane can be treated as a double-hole problem to solve the stress and displacement of the surrounding rock. As long as the number of planes selected is large enough, the stress and displacement law of the intersecting tunnel triangle can be reflected. It can be seen from Figure 2 that the shape of the tunnel section on the cutting plane is not circular. Therefore, it is necessary to use the equivalent circle method to convert the section to facilitate theoretical calculations.

2.2.1. The Complex Function Method for the Double-Hole Plane Problem. Complex functions have obvious advantages in the calculation of the stress problem of the plane porous. The method can realize the stress calculation of the plane problem with two holes under different sizes and arbitrary arrangement [15].

Schwarz alternating method provides a feasible path to calculate the stress and displacement of a double hole on a plane. The principle of this method is that assuming that there is only one hole in the plane, then the complex functions $\varphi(z)$ and $\psi(z)$ can be obtained by using the stress formula put forward by other researchers before, or the two complex functions can be gained by using the Cauchy integral method, then the stress around another hole can be calculated, and the opposite force (it is also called additional surface forces in this paper) is applied around the hole and then found the complex function corresponding to the opposite force. At this time, the excavation of the two holes has been realized. The stress of the second hole around the first hole has still to be calculated for considering the influence of the excavation of the second hole on the first hole, and then the corresponding complex function can be obtained. The iteration continues until the solution reaches a certain accuracy. By adding the complex functions, the exact solution to the existence of two holes can be obtained [16].

Chen [16] used Schwarz alternating method to describe the solution to a double hole in an infinite plane problem. And on this basis, Zhang [17, 18] and others discussed that the solution accuracy of two iterations was greatly improved compared to that of one iteration. After that, the iteration was carried out 20 times by Zhang, and the calculation results were compared with the finite element method; it was found that the calculation accuracy is enough even for two holes with a very close distance. Yan et al. [19] also used multiple methods to solve the problem of semi-infinite plane parallel tunnel in combination with series to approximate the additional surface force. Therefore, according to the results of the researchers announced, the final solution is adopted after the second iteration.

2.2.2. Equal Circle Method to Realize Cross-Sectional Shape Conversion. In this paper, the intersecting tunnels are treated as a calculation model with a circular hole and an elliptical hole in the plane. However, only the circular hole can be calculated when the complex function is solved by the Cauchy integral method. Therefore, it is necessary to map the elliptical into a circle with a complex function. In fact, it will be difficult to carry out iterative calculation after mapping, so this paper

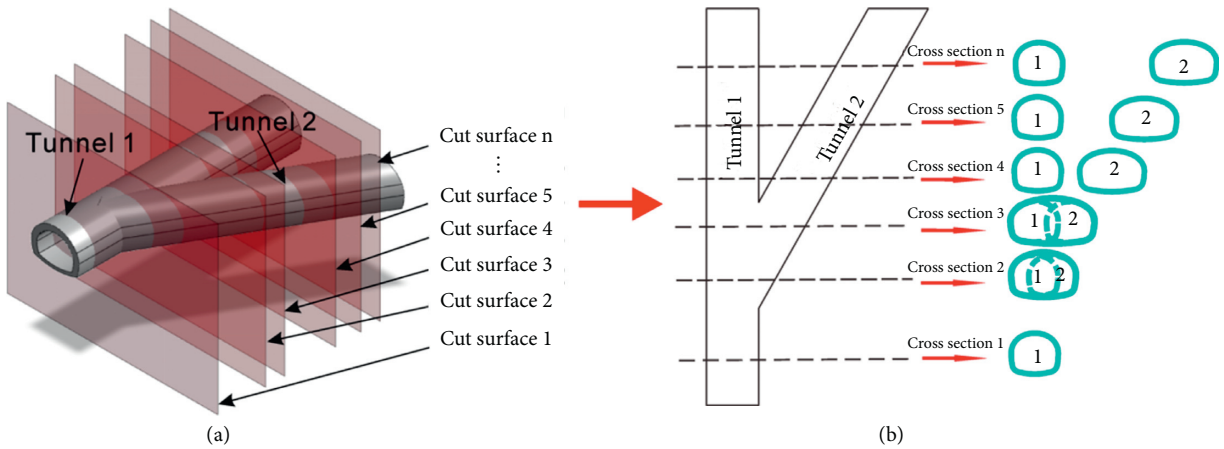

Figure 2: Simplified model of intersecting tunnels.

decides to utilize the equal circle method to convert the ellipse into the equivalent circle [18].

Tunnel sections are often round, arched wall, arched straight wall, and so on. Because of geological conditions, there are occasionally some very irregular shapes such as karst caves, cavities, and faults in underground projects. Different section forms or voids in tunnel engineering will affect the stress of surrounding rock [20, 21]. Researchers are commonly exploring the stress distribution around them by the method of mapping function which maps them to the unit circle for calculation, but the process is more cumbersome and complicated. Li [22] applied the equal circle method of the tunnel, gave the equal circle conversion method of common tunnel sections, and simplified this type of problem by using the principle of equivalence. Wu [23] and others based on the theory of the equivalent circle method and complex function studied the surrounding rock deformation and stress' diversification during the lateral expansion of a super-large-section tunnel and discussed the deformation characteristics of the surrounding rock and the width of one expansion. Peng [24] combined the field measurement and the equivalent circle method and based on conformal mapping derived the function of expressing the plastic zone radius of the surrounding rock by the anchor axial force. Under the condition of elastoplastic homogeneous surrounding rock, he obtained the radius of the plastic zone and the radius of the loose zone of the surrounding rock when the tunnel expands and analyzed the deformation characteristics of the surrounding rock; Yang [25] and others used the equivalent circle method and the Schwarz alternating method to derive the analytical solution of the surrounding rock stress during the unilateral expansion of the expanded tunnel and obtained the change law of surrounding rock displacement of the extended tunnel. Zhang [26] and others explored the construction method of noncircular tunnel stratum characteristic curve based on the theory of equivalent circle method and combined numerical analysis to obtain the best approximate analytical form.

According to the analysis of the announced research data, it is feasible to treat the cross-section form of the underground tunnel with the method of equivalent circle when analyzing the stability of the surrounding rock of the underground tunnel. Therefore, this paper deals with the section of the studied tunnel with this method.

When the tunnel section is a noncircular section such as curved wall type and straight-wall type, the complex function theory of elastic mechanics is used to calculate the surrounding rock stress and displacement. However, the calculation process of the complex function method is more complicated. In contrast, it is more convenient to calculate the surrounding rock stress of the circular tunnel section. The appearance of the equivalent circle method achieves the simplified calculation of surrounding rock stress of noncircular section, which ensures the accuracy of calculation while the calculation steps are reduced. There are usually four methods to determine the radius of an equivalent circle [27].

When the height-span ratio (h/b) is 0.8–1.25, the equivalent circle radius is as follows:

(1) Take the radius of the circumscribed circle, as shown in Figure 3(a):

$$R_d = \frac{\sqrt{h^2 + (b/2)^2}}{2\cos\left|\tan^{-1}(b/2h)\right|}. \tag{3}$$

(2) Take the radius of the arch, as shown in Figure 3(b):

$$R_d = \frac{b}{2\sin(\alpha/2)}. \tag{4}$$

(3) Take the sum of the radius, as shown in Figure 3(c):

$$R_d = \frac{a_1 + a_2}{2}. \tag{5}$$

For tunnels with large span and high side walls:

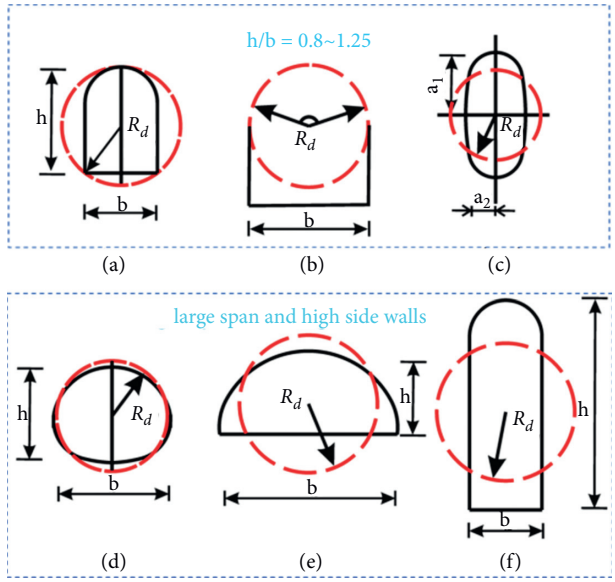

Figure 3: Calculation diagram of equivalent circle radius of different sections.

(4) Take a quarter of the sum of span and height, as shown in Figures 3(d)–3(f):

$$R_d = \frac{h+b}{4}. \tag{6}$$

In the formula, h is the section height; b is the section span.

The arched section is treated as a circle of a radius of R_d, and then the vertical stress σ_h of the triangular area of the surrounding rock of the noncircular section is obtained by formula (2).

2.2.3. Establishment of Improved Theoretical Model. After the ellipse is treated as a circle, the complex function and the Schwarz alternating method are used to solve the plane double-hole problem. Under the condition of the ideal elastic body, the complex function of the infinite plane single-hole tunnel is as follows [16]:

$$\begin{aligned}\phi_1^{(1)}(z) &= \frac{pz}{2},\\ \psi_1^{(1)}(z) &= -\frac{pa^2}{z}.\end{aligned} \tag{7}$$

After the coordinate transformation, the complex functions are changed into

$$\begin{aligned}\phi_{(1)}^{(1)}(z_1) &= \frac{pz_1}{2},\\ \psi_{(1)}^{(1)}(z_1) &= -\frac{pa^2}{z_1+c}.\end{aligned} \tag{8}$$

After applying the opposite force, the complex functions of hole 2 are as follows:

$$\begin{aligned}\phi_{(1)}^{(2)}(z_1) &= \frac{pr_1^2 z_1}{cz_1 + r_2^2} - \frac{pr_1^2}{c},\\ \psi_{(1)}^{(2)}(z_1) &= -\frac{pr_2^2}{z_1} - \frac{\rho^2}{z_1}\frac{pr_1^2 r_2^2}{\left(cz_1 + r_2^2\right)^2},\\ z\overline{z} &= \rho^2.\end{aligned} \tag{9}$$

Assuming that hole 1 is not excavated, the opposite force is applied around hole 1 after the coordinate transformation and the complex functions corresponding to the opposite force are as follows:

$$\begin{aligned}\phi_1^{(3)}(z) &= -\frac{pr_1^2 r_2^2 z^3}{\left[r_1^2 c + \left(r_2^2 - c^2\right)z\right]^2},\\ \psi_1^{(3)}(z) &= -\frac{pr_1^4 r_2^2}{\left(cz + r_2^2 - c^2\right)z} + \frac{2pr_1^2 r_2^2 z^3 \overline{z}\left(r_2^2 - c^2\right)}{\left[r_1^2 c + \left(r_2^2 - c^2\right)z\right]^3}\\ &\quad + \frac{3pr_1^2 r_2^2 z^2 \overline{z}}{\left[r_1^2 c + \left(r_2^2 - c^2\right)z\right]^2}.\end{aligned} \tag{10}$$

At this time, the excavation of the two holes is realized. Next, repeat the above steps. After the completion of the second iteration, the complex functions in the hole 1 coordinate are

$$\begin{aligned}
\phi_1(z) = {} & \frac{P_a}{4}z + \frac{p_b r_1^2}{2z} + \frac{p_b r_2^2}{2(z-c)} + \frac{p_a r_1^2 (z-c)}{2A} - \frac{p_a r_1^2}{2c} - \frac{p_b r_1^4 (z-c)^3}{2A^3} + \frac{p_b r_1^4}{2c^3} + \frac{p_b c r_1^2 (z-c)^2}{2A^2} \\
& - \frac{p_b r_1^2}{2c} - \frac{p_a r_1^2 (z-c)}{2A} + \frac{p_a r_1^2}{2c} + \frac{p_b r_1^4 (z-c)^3}{2A^3} - \frac{p_b r_1^4}{2c^3} - \frac{p_b c r_1^2 (z-c)^2}{2A^2} + \frac{p_b r_1^2}{2c} - \frac{r_1^4 r_2^2 c p_b z^3}{B^3} \\
& + \frac{r_1^4 r_2^2 c p_b}{r_2^2 - c} - \frac{r_2^2 \rho^2 p_b z^2}{2C^2} + \frac{r_2^2 \rho^2 p_b z^2}{2c^2} + \frac{r_2^2 r_1^2 \rho^2 p_a}{2B^2 C} + \frac{r_1^2 r_2^2 \rho^2 p_a}{2c\left(r_2^2 - c\right)^2} + \frac{r_1^2 r_2^2 c \rho^2 p_b z^3}{B^3} - \frac{r_1^2 r_2^2 c \rho^2 p_b}{\left(r_2^2 - c^2\right)^3} \\
& + \frac{r_2^2 p_a z}{2C} + \frac{r_2^2 p_a}{2c} - \frac{r_1^2 c p_b z}{2B} + \frac{r_1^2 c p_b}{2\left(r_2^2 - c^2\right)} - \frac{r_2^2 c p_b z}{2C} - \frac{r_2^2 p_b}{2} + \frac{r_2^2 r_1^2 c p_a z^2}{2B^2} - \frac{r_1^2 r_2^2 c p_a}{2\left(r_2^2 - c^2\right)^2},
\end{aligned}$$

$$\begin{aligned}
\phi_1^z(z) \quad & - \frac{p_a r_1^2 (z-c)}{2A} + \frac{p_a r_1^2}{2c} + \frac{p_b r_1^4 (z-c)^3}{2A^3} - \frac{p_b r_1^4}{2c^3} - \frac{p_b c r_1^2 (z-c)^2}{2A^2} + \frac{p_b r_1^2}{2c} - \frac{r_1^4 r_2^2 c p_b z^3}{B^3} \\
& + \frac{r_1^4 r_2^2 c p_b}{r_2^2 - c} - \frac{r_2^2 \rho^2 p_b z^2}{2C^2} + \frac{r_2^2 \rho^2 p_b z^2}{2c^2} + \frac{r_2^2 r_1^2 \rho^2 p_a}{2B^2 C} + \frac{r_1^2 r_2^2 \rho^2 p_a}{2c\left(r_2^2 - c\right)^2} + \frac{r_1^2 r_2^2 c \rho^2 p_b z^3}{B^3} - \frac{r_1^2 r_2^2 c \rho^2 p_b}{\left(r_2^2 - c^2\right)^3} \\
& + \frac{r_2^2 p_a z}{2C} + \frac{r_2^2 p_a}{2c} - \frac{r_1^2 c p_b z}{2B} + \frac{r_1^2 c p_b}{2\left(r_2^2 - c^2\right)} - \frac{r_2^2 c p_b z}{2C} - \frac{r_2^2 p_b}{2} + \frac{r_2^2 r_1^2 c p_a z^2}{2B^2} - \frac{r_1^2 r_2^2 c p_a}{2\left(r_2^2 - c^2\right)^2},
\end{aligned}$$

$$\begin{aligned}
\psi_1(z) = {} & -\frac{p_b z}{2} - \frac{p_a r_1^2}{2z} + \frac{p_b r_1^4}{2z^3} - \frac{\rho^2}{z-c}\left[-\frac{r_2^2 p_b}{2(z-c)} + \frac{r_1^2 r_2^2 p_a}{2A^2} - \frac{3 r_1^4 r_2^2 p_b (z-c)^2}{2A^4} + \frac{r_1^2 r_2^2 c p_b (z-c)}{A^3}\right] \\
& - \frac{r_2^2 p_a}{2(z-c)} - \frac{r_1^2 p_b (z-c)}{2A} + \frac{r_1^2 p_b}{2c} - c\left[-\frac{r_2^2 p_b}{2(z-c)} + \frac{r_1^2 r_2^2 p_a}{2A^2} - \frac{3 r_1^4 r_2^2 p_b (z-c)^2}{2A^4} + \frac{r_1^2 r_2^2 c p_b (z-c)}{A^3}\right] \\
& - \frac{3 r_1^2 r_2^4 p_b}{c^3 B} + \frac{r_1^2 r_2^6 p_b z^2}{c^3 B^2} - \frac{r_2^2 p_b z}{C} + \frac{r_1^2 C p_a}{B} + \frac{r_1^4 C^3 p_b}{B^3} - \frac{r_1^2 C^2 c p_b}{B^2} - \frac{\rho^2}{z}\phi_1^{z'}(z) + \frac{r_1^2}{z}\left[\frac{r_2^2 p_b}{2(z-c)^2} - \frac{r_1^2 r_2^2 p_a}{2A^2} + \frac{3 r_1^4 r_2^2 (z-c)^2 p_b}{2A^4} - \frac{r_1^2 r_2^2 c (z-c)^2 p_b}{B^3}\right].
\end{aligned} \tag{11}$$

Based on the relationship between the complex function and the stress, the stress and displacement around the double-hole tunnel can be obtained:

$$\begin{aligned}
\sigma_\rho + \sigma_\theta &= 4\mathrm{Re}\left[\phi_1'(z)\right], \\
\sigma_\theta - \sigma_\rho + 2i\tau_{\rho\theta} &= 2e^{2i\theta}\left[\overline{z}\phi_1''(z) + \psi_1(z)\right], \\
2G(u+iv) &= k\phi(z) - z\overline{\phi'}(z) - \overline{\psi}(z).
\end{aligned} \tag{12}$$

In the formula, $\phi_1^{(1)}(z)$ and $\psi_1^{(1)}(z)$ are the complex functions after the excavation of hole 1 under the coordinates of hole 1; $\phi_{(1)}^{(1)}(z)$ and $\psi_{(1)}^{(1)}(z)$ are the form of complex functions that transform the coordinates of hole 1 to the coordinate of hole 2; $\phi_{(1)}^{(2)}(z)$ and $\psi_{(1)}^{(2)}(z)$ are the complex functions of the opposite force applied around the hole 2 in the coordinate of hole 2 (the excavation of the hole 2); $\phi_1^{(3)}(z)$ and $\psi_1^{(3)}(z)$ are the complex functions of opposite force applied around the hole 1 in the coordinate of hole 1; $\phi_1(z)$ and $\psi_1(z)$ are complex functions as the final solution; P is the original rock stress; z is the complex coordinate, $z = x + yi$; $\overline{z}$ is the conjugate complex number of z, $\overline{z} = x - yi$; C is the distance between the centers of the two holes; r_1 and r_2 are the radius of hole 1 and hole 2, respectively; $p_a = p_1 + pp_2$ and $p_b = p_2 - p_1$, when $\lambda = 1$; vertical stress and horizontal stress are equal; $p_a = 2p$ and $p_b = 0$; $A = r_{22} - c_2 + zc$, $B = (r_{22} - c_2)z + r_{12}$, and $C = r_{12} - zc$.

The theoretical model has been fully described by the above content. The flowchart of the theoretical model algorithm is shown in Figure 4. In the next section, the final iterative calculation formulas $\phi_1(z)$ and $\psi_1(z)$ will be written as code and input into the Matlab program to calculate the stress in the triangular area of the intersection tunnel with different cross sections.

3. Calculation Example Verification and Physical Engineering Analysis

In order to verify the rationality of the theoretical calculation models used in the tunnel intersection, two numerical model cases (the stress and displacement of surrounding rock were verified separately) and an indoor model test (test monitoring of the surrounding rock stress was verified) are selected to analysis comparatively. Based on the physical engineering in Guiyang City, the analysis and discussion on the influence of section differences on the stress distribution law in the triangle area were carried out.

3.1. Calculation Example Verification 1. Zhao et al. [28] conducted a numerical simulation study on the influence of the principal stress in the intersecting roadway on the stability of the surrounding rock at the intersection and selected a section on-site to monitor the deformation of the surrounding rock within 30 days of excavation. The cross section of the intersecting roadway is an arched straight wall. The roadway is 4.8 m wide and 3.5 m high. The shear modulus of the rock mass is 0.45 GPa, and the bulk modulus is 1.43 GPa. The vertical principal stress is 5.8 MPa. Besides, the average maximum horizontal stresses and the minimum horizontal stress of the in situ stress are 7.52 MPa and 6.36 MPa which can correspond to the values of P_2 and P_1 in the theoretical model of this paper. After the straight-wall section is converted into a circular section by the equivalent circle method, the section radius $r = 2.573$ m. Figure 4 shows the comparison between the stress complex function method of surrounding rock, the single-tunnel superposition calculation method, and the numerical simulation stress results given by Zhao which considered the mutual influence of the cross tunnel excavation.

It can be seen from Figure 5 that the surrounding rock stress calculated by the model put forward from this paper and the stress value curve given by the example both show a change that first increases and then decreases. The single-hole superposition method is ideally represented as the closer it is from the center of the excavation surface, the greater the stress values are. Therefore, with the calculation point principle, the excavation surface shows a gradual decrease, and there is no increasing change curve, which cannot show that the surrounding rock may be damaged. However, in actual engineering tunnel excavation, there will be areas of increased and decreased stress [29], so the calculation method of direct superimposed stress is not applicable.

From the comparison between the theoretical model of this paper and the calculation results of this paper, due to the difference between the processing of the numerical model and the theoretical calculation, it can be seen that the peak value and rate of change of the two are different, but they both tend to the original rock stress in the end. Due to the impact on excavation, the area affected by the surrounding rock is roughly the same. The stress rise area is 8 m from the intersection. In this range, the phenomenon that the plastic surrounding rock or even the surrounding rock is damaged due to the stress exceeding the uniaxial compressive strength of the rock masses is more likely to occur. When the distance is 8–14 m from the intersection, the stress will recover, and the stress will gradually decrease and stabilize. The above analysis shows that the changes of the two are similar and the error is small, so the theoretical calculation method proposed in this paper is suitable for this project.

3.2. Calculation Example Verification 2. Li [30] and others adopted numerical simulation excavation and selected measured points on-site to explore the stress and deformation of surrounding rock in the intersection, in view of the fact that the subway tunnel and the station formed a typical large-section and small-section intersection, and the centers of the two sections were not on the same level plane. According to the paper description, the large section is round arch, 17.45 m of high and 22.10 m of wide, the small section is arched straight-wall type, 6.6 m of high and 8.0 m of wide, and the intersection angle is 90°. After converting the section to an equivalent circle, the large cross-section equivalent circles $r1 = 9.89$ m and $r2 = 4.54$ m, so the vertical height difference between the two circle centers is $h = 5.35$ m.

Figure 6 shows the comparison between the calculation method of the theoretical model, the single-cavity stacking method, and the settlement calculation results of the large-section vault given in the paper. The calculation result of the single-cavity stacking method of Figure 6 shows that the settlement decreases as the distance increases and tends to be stable, but its overall settlement value differs greatly from the calculation result from the article. This is due to the mutual excavation of the cross tunnels, and the surrounding rock is disturbed more and more times of different degrees than in the single-hole excavation. The final vertical displacement is greater than that of directly superimposing the settlement of two single holes [14]. Therefore, the single-hole superposition method still cannot provide theoretical guidance on settlement issues.

Compared with the deformation value given in the article and the theoretical deformation value calculated from the model in this paper, it shows that the initial deformation of the theoretical value is larger, and the value of the distance from the intersection after stable deformation is larger (about 20 m). The article gives the stable displacement as about 14 m; this is related to the support treatment of the model carried out by the author of the article, which makes the surrounding rock safer, but the deformation curve changes calculated by the comparison between the two are similar and relatively close. As the distance between the calculated point and the intersection becomes larger and larger, the theoretical calculation and the surrounding rock deformation value given in the article generally show a decreasing change pattern, but the data in the article shows that, within a short distance (within 6 m), the rate of deformation decrease is greater than other distance values, and the rate of change in the range of 8–14 m decreases and tends to 10 mm. From the comparison and analysis of the above two, it can be considered that the theoretical calculation method proposed in this paper has a more accurate theoretical reference to similar tunnel projects than the single-hole superposition method.

3.3. Calculation Example Verification 3. A similar model experiment was carried out by Dong to explore the stress change and settlement deformation laws in the bottom of the existing tunnel and the surrounding rock above the new tunnel when the new tunnel underpasses the existing heavy-duty railway tunnel [31]. The project is a spatial cross tunnel. The bottom of the existing tunnel at the upper part is 16 m from the vault of the new tunnel at the lower part. The two tunnels have the same cross section, with a span of 14 m, a

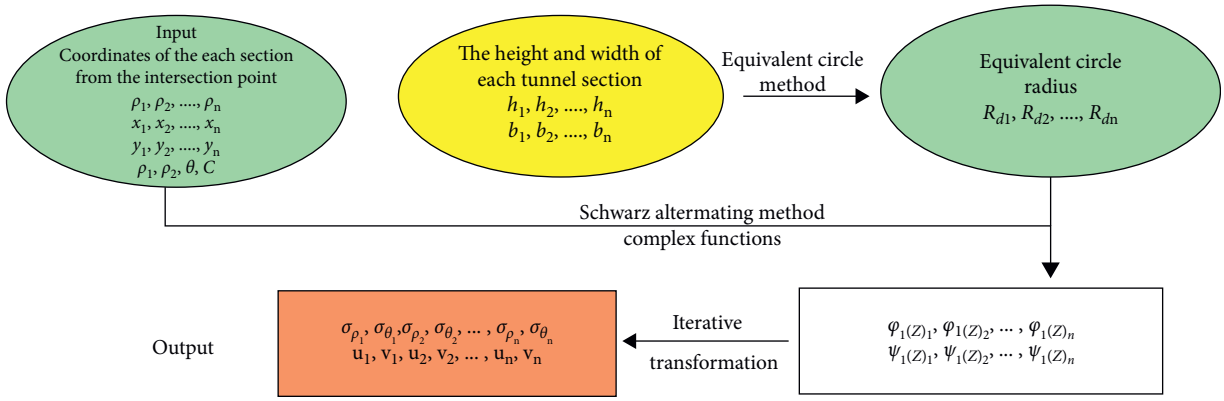

Figure 4: Algorithm flowchart of the theoretical model.

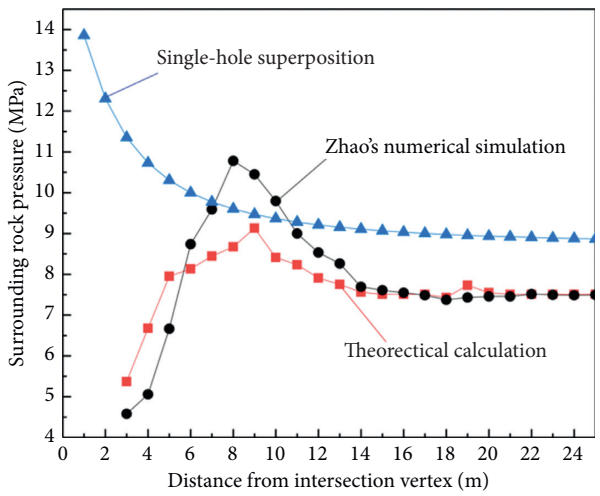

Figure 5: Comparison of calculation results of surrounding rock deformation.

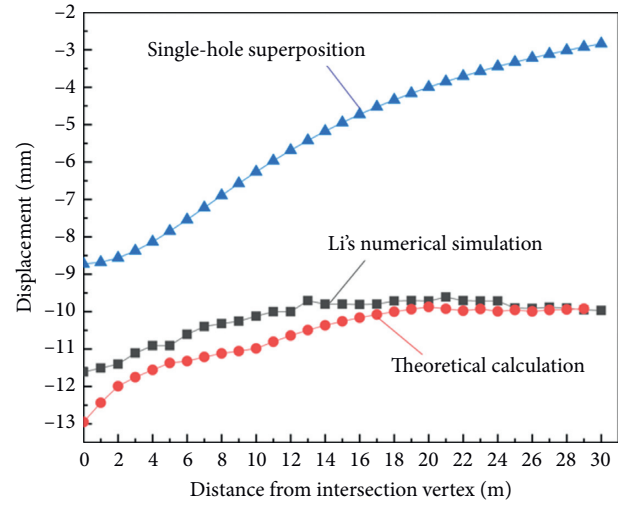

Figure 6: Comparison of calculation results of surrounding rock deformation.

height of 11.8 m, and a crossing angle of 76°. The surrounding rock of the upper tunnel is mainly strongly weathered tuff, and the surrounding rock of the lower tunnel is mainly medium weathered tuff. Dong preembeded the stress box of the bottom of the existing tunnel and placed it along the tunnel with a longitudinal spacing of 20 cm. At the same time, the stress monitoring points were arranged at the intersection of the existing tunnel and the new tunnel with a vertical spacing of 8 cm.

Based on the author's test stress results, this paper applies the single-cavity superposition method and the model calculation method in this paper to its model test conditions, calculates the surrounding rock stress, and compares the measured value of the test stress. The comparison result curve is shown in Figure 7. It can be seen from Figure 7 that two calculation methods show similar laws. As the increase of distance to the intersection, the stress of points in the existing tunnel bottom gradually increases from negative to positive and tends to stabilize, while the measured data of the experiment also increases with the increase of the distance. However, after considering the mutual influence of the cross tunnel excavation, the theoretical calculation model in this paper is closer to the measured value. This is because the mutual influence of the cross tunnel excavation affects the surrounding rock more frequently and the surrounding rock is more dangerous. At the same time, it can be seen that tensile stress of 25 kPa appears at the bottom of the existing tunnel due to the excavation of the new tunnel at the intersection. From the perspective of the change trend, the tensile stress of the surrounding rock decreases due to the gradually moving away from the intersection and the transition to a safe state, until the distance is 15 cm; the force of the model material does not turn into compressive stress and continues to increase to 13 kPa.

The measured value of the stress at the intersection reached 31 kPa. As the distance increases, the tensile stress decreases and turns to compressive stress. The model calculation in this paper is basically consistent with the measured results. Therefore, the theoretical calculation method proposed in this paper can be used as the theoretical curve of the experimental stress test results. However, the single-hole superposition method is obviously difficult to guide the test stress, mainly because the stress curve is relatively stable, and it does not reflect the change of the experimental stress test results.

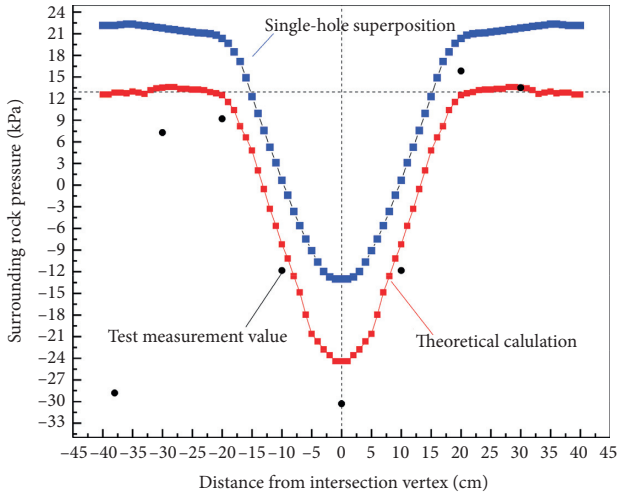

Figure 7: Comparison between calculation results of surrounding rock pressure and test measurement.

3.4. Physical Engineering Analysis. In order to make full use of the existing underground structure, it is planned to expand on the original foundation. In the expansion project of an underground civil air defense tunnel in Guiyang City, the expanded tunnel intersects the existing tunnel at 90°, the two tunnels are quite different in section, and the section of the tunnel is arched straight-wall type. The existing tunnel has a cross-sectional span of 8.9 m, a height of 6.95 m, and a burial depth of 22.65 m. From the surface to the vault of the existing tunnel, there are three types of rock and soil, and their bulk densities are $\gamma_1 = 17.1\text{kN/m}^3$, $\gamma_2 = 27\text{kN/m}^3$, and $\gamma_3 == 27.5\ \text{kN/m}^3$. Based on the equivalent circle method, the cross sections of the extended tunnel and the existing tunnel are converted into circles. In this section, the stress of surrounding rock under four crossing angles was calculated (30°, 45°, 80°, and 90°). In order to reflect whether the centers of the intersecting tunnels are in the same plane, it is set when the radius is equal ($r_1 = 1.0r_2$) that the center of the circle is in the same plane; the centers of the circles are not in the same plane for calculation ($r_1 = 2.0r_2$, $r_1 = 3.0r_2$, and $r_1 = 4.0r_2$) when the cross sections are different.

3.4.1. Analysis of the Influence of the Angle between the Intersecting Tunnels on the Stress Distribution of the Surrounding Rock. It can be seen from Figure 8 that the stress concentration of the surrounding rock in the triangle area gradually decreases (the stress of the surrounding rock tends to the original rock stress) with the increase of the intersection angle of the intersecting tunnels (30° to 90°). Under different tunnel diameter differences, the most dangerous situation is the 30° intersection angle (tensile stress occurs in the surrounding rock), but with the increase of the intersection angle, the change rate of the surrounding rock stress which tends to be the original rock stress is increasing, which shows that the surrounding rock becomes safer. Therefore, in the case of different angles, the 90° intersection angle is the safest. And the surrounding rock gradually becomes stable with the increase in calculation distance.

3.4.2. Analysis of Influence of Tunnel Diameter Difference on Surrounding Rock Stress Distribution. Some points of the angle bisector of the triangle area are selected for calculation. It can be seen from Figure 9 that, under the same intersection angle, the stress change of the surrounding rock at the same point increases first and then decreases with the increase in the size difference of the cross section of the intersecting tunnels. Within the influence range of stress concentration, the surrounding rock with a difference of twice the hole diameter is the most dangerous under different intersection angle. At the same time, it can be seen that as the stress is distributed from the shallow part to the deep part of the rock mass, the same trend appears. The phenomenon of that is consistent with the inference put forward by the literature [32]; that is, the stress of surrounding rock does not only decrease with the increase of the distance from the intersection center, but there is peak stress between the shallow and deep surrounding rock.

3.4.3. Monitoring Experiment in Construction Site. In order to ensure the stability of the surrounding rock during the construction of the project, six detectors were buried at the most dangerous intersection (twice the section diameter), to monitor the vault and arch toe of the section, as shown in Figures 10(a)–10(c). The monitoring results have been shown in Figure 10(d). It can be seen from the figure that the time for the surrounding rock stress to stabilize is 50 days, except for the arch toe of the surrounding rock with a large section later than other places (about 70 days). And the stress tends to stabilize to the maximum (about 0.7 MPa). The size of the excavated section of the existing tunnel is half the size of the new tunnel, so the arch toe of the large section is more disturbed and more frequently during the construction. The maximum stress of the small-section tunnel appears in the vault, which is about 0.48 MPa, while the arch toe on both sides is about 0.4 MPa which is different from the large-section tunnel.

Compared with theoretical calculations, the results of on-site monitoring are safer (mainly manifested as smaller stress), which is related to the theory that only considers tunnel excavation without considering the supporting structure. On-site monitoring results are consistent with the laws of theoretical analysis.

3.4.4. Three-Dimensional Numerical Model. In order to verify the calculation results of the theoretical model, the Midas-GTS 3D FEM software was used and some numerical models of the expansion project were created under the same conditions of theoretical calculation. Most of the tunnels are under the moderately weathered dolomite. The Mohr-Coulomb constitutive model based on the

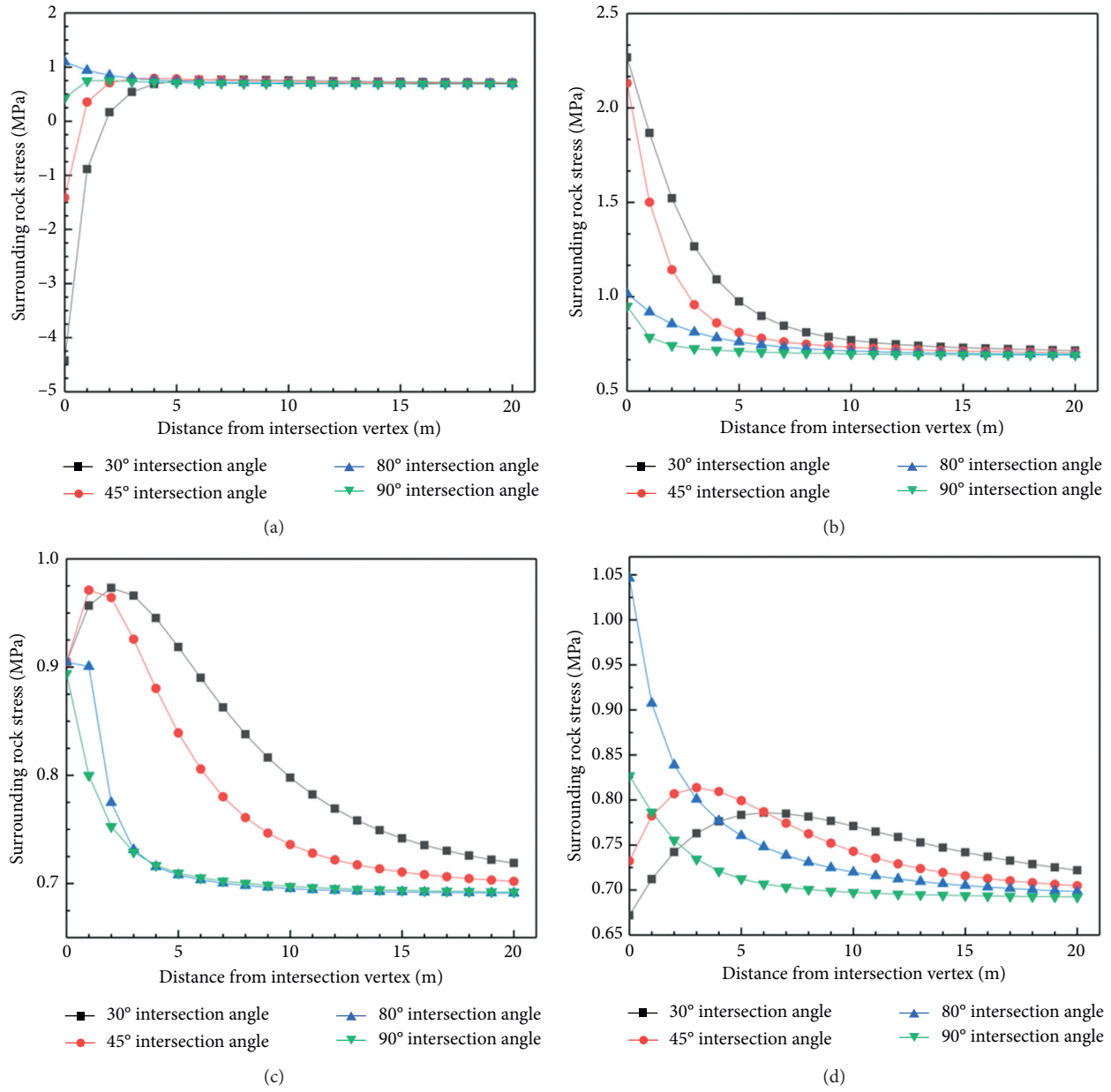

Figure 8: Stress variation of surrounding rock under different tunnel diameters differences. (a) Once the hole diameter; (b) twice the hole diameter; (c) 3 times the hole diameter; (d) 4 times the hole diameter.

continuum is adopted. The intersecting tunnels with the same diameter (width of 8.9 m; high of 6.95 m) and twice the diameter of the section are selected to compare the stress of surrounding rock on the angle bisector of the triangle area under the angles of 30°, 45°, and 90°. Two of those numerical models are shown in Figures 11(a) and 11(b) as typical representative. In order to consider the impact of tunnel excavation, the model is set to be 91 m high and 100 m long, and the width is taken as the expansion project length of 80 m. The rock mass mechanical parameters are shown in Table 1. The comparison of calculation results is shown in Figure 12.

From the comparison between the numerical simulation calculation and the theoretical model calculation in this paper, as shown in Figure 12, it can be seen that the calculation results of the surrounding rock stress in the triangle area of the two show similar laws. In Figure 12(a) with once the hole diameter, the different intersection angles gradually tend to the original rock stress after 5 m.

In Figure 12(b) with twice the hole diameter, the numerical simulation results tend to the original rock stress after 15 m only when the intersection angle is 90°. Compared with once the diameter of the cave, the rate at which the surrounding rock tends to the original rock stress

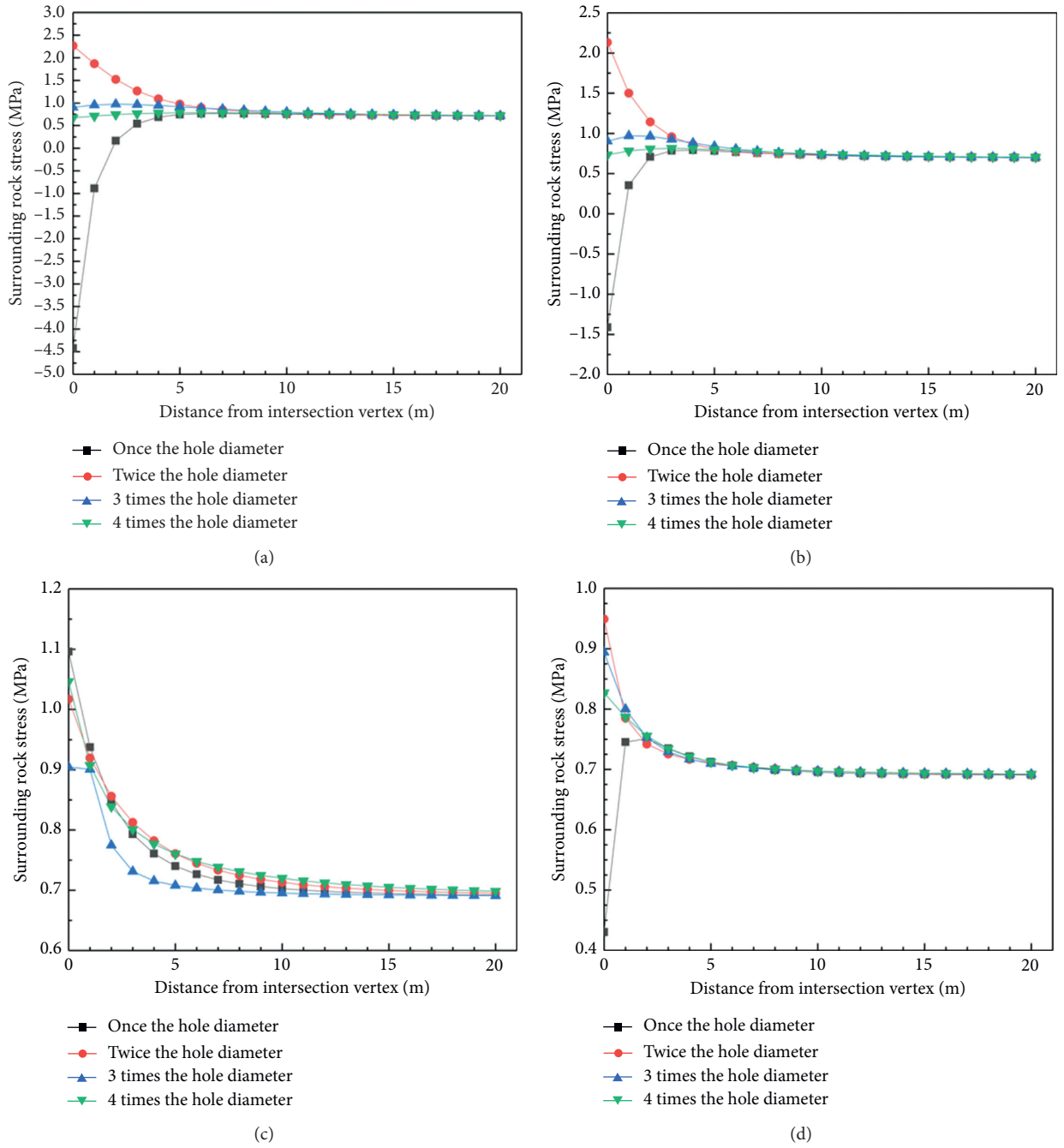

Figure 9: Stress variation of surrounding rock under different angle. (a) 30-degree angle; (b) 45-degree angle; (c) 80-degree angle; (d) 90-degree angle.

becomes smaller, and the theoretical calculation gradually tends to the original rock stress after 7 m. Both calculation results show that, in the range of 0–5 m from the intersection point, the stress caused by the excavation of the surrounding rock is higher, and the rate of change is greater, indicating that the surrounding rock in this range is more dangerous than other places. In the range of 5–10 m, the stress reduction rate becomes smaller, which means that the surrounding rock becomes safer. This is the secondary stress redistribution phenomenon self-adjusting after the excavation of the rock mass. This phenomenon reflects the rock mass as a characteristic of the main burden of the load and the source of the load. The surrounding rock at each intersection angle of once the hole diameter is in the original rock stress state after 10 m, but under twice the hole diameter, only 90° intersection angle that is safe after 6 m through theoretical calculation. The intersection angles of the numerical simulation tend to be safe mainly after

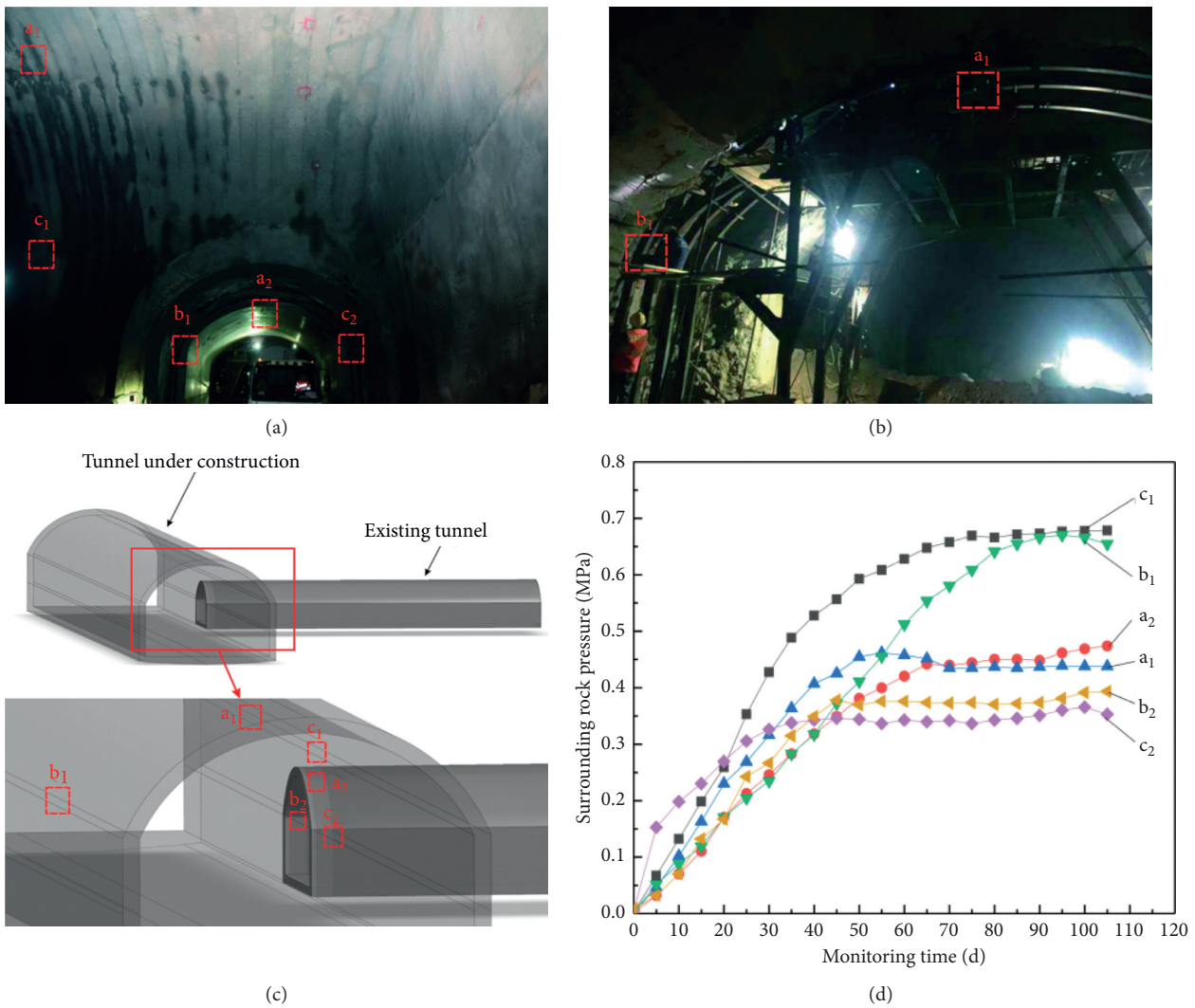

Figure 10: Monitoring data of surrounding rock at tunnel intersection. (a) Small-section monitoring point on-site; (b) large-section monitoring point on-site; (c) monitoring point layout model; (d) monitoring data on-site.

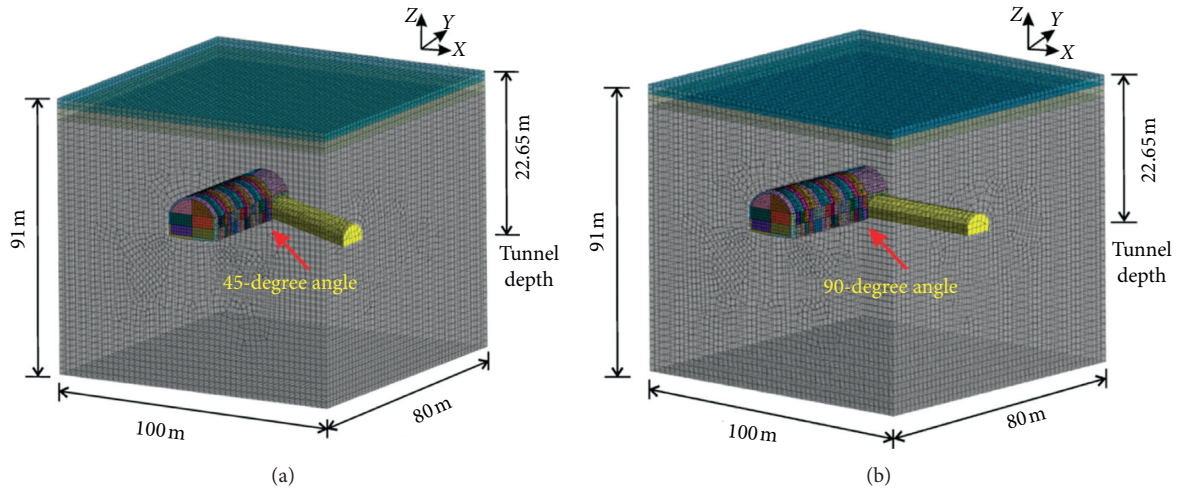

Figure 11: Three-dimensional numerical model. (a) Twice the hole diameter with a 45-degree angle. (b) Twice the hole diameter with a 90-degree angle.

Table 1: Mechanical parameters of rock mass.

	Elastic modulus (MPa)	Poisson's ratio	Bulk density (kN/m^3)	Cohesion (kN/m^2)	Friction angle (°)
Red clay	18.1	0.33	17.1	30	10
Strongly weathered dolomite	1000.0	0.18	27.0	100	25
Moderately weathered dolomite	2500.0	0.15	27.5	300	30
Spray mixing	28000.0	0.20	25.0	/	/

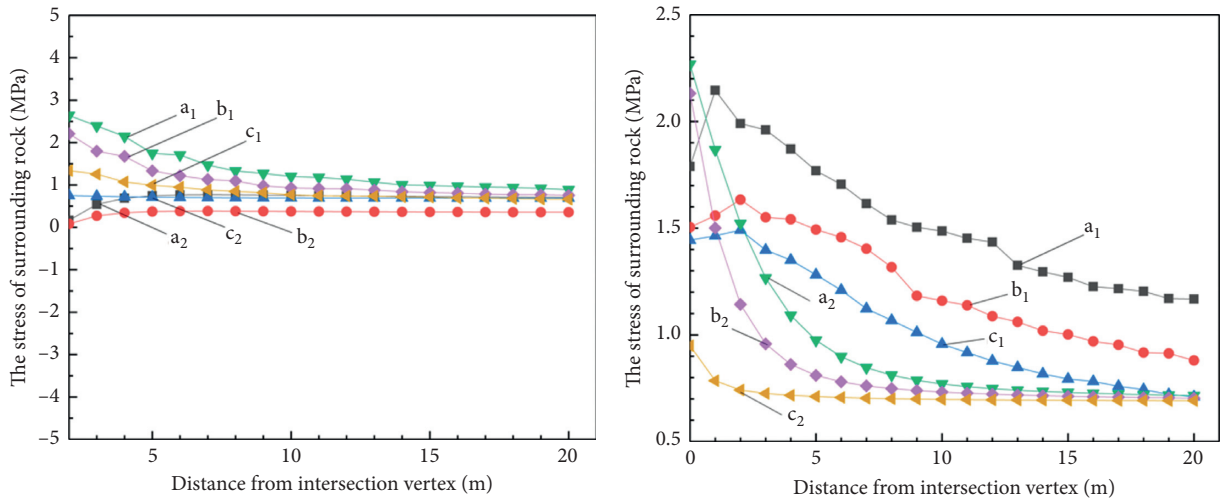

Figure 12: Results of numerical simulation and theoretical model. a_1–c_1: numerical simulation of 30°, 45°, and 90° intersection angle; a_2–c_2: theoretical model of 30°, 45°, and 90° intersection angle; (a) once the hole diameter; (b) twice the hole diameter.

20 m, but the 90° intersection angle condition is the first to be in a safe state, which shows that the orthogonal way is the safest structural method of the cross tunnel. The above comparison shows that the theoretical calculation and numerical simulation calculation are consistent in describing the law of stress in the surrounding rock of the intersecting tunnel. Therefore, the theoretical calculation in this paper can provide a reference to similar projects.

4. Conclusion

(1) With the help of the complex function and the alternating method, the calculation of the stress of the surrounding rock of the intersecting tunnel is simplified to a plane model without considering the influence of longitudinal excavation. This paper calculated and obtained that when the angle of the intersecting tunnel triangle area is 30°–90°, it is safe when the distance from the intersection vertex is at least 10 m away. By this time, the requirement of the surrounding rock support can be reduced according to the situation.

(2) As the increase of the intersection angle of the tunnel, the surrounding rock stress tends to stabilize because of the increase of the change rate which tends to the original rock stress. When the intersection angle increased to 90° the surrounding rock stress was the safest.

(3) With the increase of the diameter difference between the intersecting tunnels, the surrounding rock stress first increases and then decreases. However, the larger difference in tunnel diameter has a wider range of influence than the smaller difference in tunnel diameter.

(4) Compared with the direct superposition shear stress of single-hole superposition theory, the theoretical calculation models that take into account the mutual influence of cross tunnel excavation are closer to stress regular pattern in reality and that can be used as a reference to underground engineering under complex conditions in the future.

Data Availability

The data used to support the findings of this study are available from the corresponding author upon request.

Conflicts of Interest

The authors declare that they have no conflicts of interest.

Acknowledgments

The authors gratefully acknowledge the support from the projects funded by the Guizhou Province Basic Research Project ([2020]1Y250), China Postdoctoral Science Foundation (No. 2017M622929), Guizhou Province Science and

Technology Support Plan Project ([2020]2Y036), Guizhou University Talent Introduction Research Project (GDRGHZ(2017)62), Guangxi University Open Project(2016ZDK012) and Guizhou Province Civil Engineering First Class(QYNYL[2017]0013).

References

[1] Z. Liu, "Control technology of surrounding rock at large section non-equal height intersection," Dissertation, China University of Mining & Technology, Xuzhou, China, 2019.

[2] S. Ping, M. Liu, and R. Zhang, "Stability analysis of surrounding rock at intersection - Study on Mechanism of roadway roof accident," *Ground Pressure and Roof Management*, vol. 1, pp. 33–39, 1990.

[3] L. Sun, "Study on the surrounding rock stability characteristics and control methods in the roadway junction," Dissertation, Taiyuan University of Technology, Taiyuan, China, 2014.

[4] J. Rao, C. Xie, X. Zhao, D. Liu, C. Nie, and N. Liu, "Theoretical stability calculation of surrounding rocks in divergence of deep tunnel," *Journal of Central South University (Science and Technology)*, vol. 50, no. 8, pp. 1949–1959, 2019.

[5] T. Shi, "Surrounding rock deformation law and support calculation method of roadway intersection," *Design and Construction of Metallurgical Mines*, vol. 5, pp. 7–11, 1994.

[6] R. N. Singh, I. Porter, and J. Hematian, "Finite element analysis of three-way roadway junctions in longwall mining," *International Journal of Coal Geology*, vol. 45, no. 2-3, pp. 115–125, 2001.

[7] Y. R. Chugh and B. Abbasi, "A numerical analysis of a four-way coal mine intersection with primary and secondary supports," in *Proceedings of the Harmonising Rock Engineering and the Environment—Proceedings of the 12th ISRM International Congress on Rock Mechanics*, The Chinese Society for Rock Mechanics and Engineering, The Society for Rock Mechanics & Engineering Geology Singapore, Beijing, China, October 2011.

[8] P. Yoginder, "Numerical modeling of roof support plans at 4-way coal mine intersections," in *Proceedings of the 49th U.S. Rock Mechanics Geomechanics Symposium*, American Rock Mechanics Association, San Francisco, California, June 2015.

[9] H. Wu, G. Zhao, W. Liang, E. Wang, and S. Ma, "Experimental investigation on fracture evolution in sandstone containing an intersecting hole under compression using DIC technique," *Advances in Civil Engineering*, vol. 2019, Article ID 3561395, 12 pages, 2019.

[10] C. Liu, L. Peng, M.-F. Lei, and Y.-F. Li, "Research on crossing tunnels' seismic response characteristics," *KSCE Journal of Civil Engineering*, vol. 23, no. 11, 2019.

[11] M. Lei, D. Lin, Q. Huang, C.-H. Shi, and L. Huang, "Research on the construction risk control technology of shield tunnel underneath an operational railway in sand pebble formation: a case study," *European Journal of Environmental and Civil Engineering*, vol. 24, no. 5, pp. 1–15, 2020.

[12] M. Lei, J. Liu, Y. Lin, C. Shi, C. Liu, and T. Saksala, "Deformation characteristics and influence factors of a shallow tunnel excavated in soft clay with high plasticity," *Advances in Civil Engineering*, vol. 2019, Article ID 7483628, 14 pages, 2019.

[13] M. Lei, L. Liu, Y. Lin et al., "Experimental investigation of damage evolution characteristics of C50 concrete under impact load," *Shock and Vibration*, vol. 2020, Article ID 2749540, 10 pages, 2020.

[14] M. Shen and J. Chen, *Rock Mechanics*, Tongji University Press, Shanghai, China, 2015.

[15] Z. Zhang, C. Zhang, and X. Xi, "Closed solutions to soil displacements induced by twin-tunnel excavation under different layout patterns," *Chinese Journal of Geotechnical Engineering*, vol. 41, no. 2, pp. 262–271, 2019.

[16] Z. Chen, *Analytical Methods in Analysis of Rock mechanics*, China Coal Industry Publishing House, Beijing, China, 1994.

[17] L. Zhang and A. Lv, "Study on alternating method for stress analysis of surrounding rock of double hole circular tunnel," *Chinese Journal of Rock Mechanics and Engineering*, vol. 5, pp. 56–65, 1998.

[18] L. Zhang, Z. Yang, and A. Lu, "Study on the plane elasticity of two holes with arbitrary shape under arbitrary arrangement," *Scientia Sinica (Terrae)*, vol. 5, pp. 509–518, 2000.

[19] L. Yan, J. Yang, and B. Liu, "Stress and displacement of surrounding rock with shallow twin-parallel tunnels," *Chinese Journal of Geotechnical Engineering*, vol. 33, no. 3, pp. 413–419, 2011.

[20] X. Hao, S. Wang, D. Jin et al., "Instability process of crack propagation and tunnel failure affected by cross-sectional geometry of an underground tunnel," *Advances in Civil Engineering*, vol. 2019, Article ID 3439543, 17 pages, 2019.

[21] H. W. Chen and C. Sha, "Stability analysis of surrounding rock and treatment structures in superlarge karst cave of naqiu tunnel," *Advances in Civil Engineering*, vol. 2018, Article ID 4842308, 14 pages, 2018.

[22] S. Li, *New Theory of Tunnel Support Design (Application and Theory of Typical Analogy Analysis Method)*, China Water Resources and Hydropower Press, Beijing, China, 2002.

[23] Z. Wu, G. Xu, L. Wu, and Y. Qian, "Mechanical deformation characteristics of rock mass surrounding lateral enlarging excavation of tunnels with ultra-large sections," *Chinese Journal of Geotechnical Engineering*, vol. 31, no. 2, pp. 172–177, 2009.

[24] N. Peng, "Study on surrounding rock mechanical response mechanism of in-situ enlarged tunnel," Dissertation, Chongqing University, Chongqing, China, 2010.

[25] B. Yang, C. Lin, Z. Zhang, R. Yin, and Z. Wen, "Mechanical characteristics analysis of surrounding rock of unilateral expansion tunnels in situ," *Chinese Journal of Underground Space and Engineering*, vol. 14, no. 6, pp. 1458–1465, 2018.

[26] P. Zhang, Y. Su, K. Wang, Z. Luo, and W. He, "An approximate building method of ground reaction curve for non-circular underground tunnels," *Hydrogeology & Engineering Geology*, vol. 42, no. 2, pp. 52–58, 2015.

[27] Y. Su, H. E. Manchao, and Q. Gao, "Application of Rosenblueth method in evaluating stability reliability of anchor-shotcrete net support system for soft-fractrue surrounding rock," *Chinese Journal of Geotechnical Engineering*, vol. 3, pp. 378–382, 2004.

[28] W. Zhao, L. Han, Z. Zhao, Q. Meng, and H. Liu, "Influence of principal stress on surrounding rock stability of roadway intersection," *Rock and Soil Mechanics*, vol. 36, no. 6, pp. 1752–1760, 2015.

[29] M. Qian and P. Shi, *Mine Pressure and Rock Formation Control*, pp. 47–58, China University of Mining and Technology Press, Xuzho, China, 2003.

[30] Y. Li, X. Jin, Z. Lv, J. Dong, and J. Guo, "Deformation and mechanical characteristics of tunnel lining in tunnel intersection between subway station tunnel and construction tunnel," *Tunnelling and Underground Space Technology*, vol. 56, pp. 22-23, 2016.

[31] J. Dong and S. Zhong, "Influence of under-crossing on the rock stress of pillar between crossing tunnels," *Journal of Railway Science and Engineering*, vol. 17, no. 4, pp. 947–956, 2020.

[32] W. Zhao, L. Han, and Y. Zhang, "Study on the change law of disturbance principal stress and the stability of surrounding rock of vertical working intersection," *Journal of Mining & Safety Engineering*, vol. 32, no. 1, pp. 90–98, 2015.